



A Novel Barrier Function Adaptive Terminal Sliding Mode Controller for Trajectory Tracking of a Nonholonomic Wheeled Mobile Robot

Fahimeh Kordi¹, Hamidreza Alikhani^{*2}, Javad Nikoukar¹

¹ Department of Technical Engineering, Faculty of Engineering, Saveh Branch, Islamic Azad University, Saveh, Iran.

² Department of Technical Engineering, Faculty of Engineering, Tafresh University, Tafresh, Iran.

Received: 09-Jan-2024, Accepted: 12-Apr-2024.

Abstract

This paper introduces and discusses a new control strategy for nonholonomic wheeled mobile robots (WMR). Robot models include kinematic and dynamic equations of motion. A barrier function adaptive terminal sliding mode control is used to control the movement of the robot. It considers sliding mode control (SMC) to deal with the dynamic model uncertainties of the chaos system and uses a combination of SMC with an adaptive control approach to solve the upper boundaries problem of unknown model uncertainties and their estimation. Chattering is completely eliminated without over-estimating the control gains by adopting an adaptive continuous barrier function in the dynamic switching function. Using Lyapunov's stability theory, it was shown that the proposed scheme can guarantee the convergence of system states to the vicinity of the sliding surface in finite time. Additionally, the adoption of a sliding surface with a nonlinear and integral switching function resulted in removing the reaching phase of the sliding surface and yielding a controller that is robust to uncertainties from the start. The effectiveness of the proposed control method was assessed using three scenarios implemented to Liu's uncertain chaotic system in a MATLAB/Simulink environment. The obtained results confirmed the ability of the proposed approach to achieve continuous and smooth control rules for such chaotic systems. Among the main attributes of the proposed control method is its ability to completely eliminate chattering and yield a robust performance against model uncertainties and unknown external disturbances.

Keywords: Nonholonomic Wheeled Mobile Robot, Adaptive Barrier Function, Terminal Sliding Mode Control, Trajectory Tracking, Chattering-Free.

*Corresponding Authors Email:
alikhani.hamid@gmail.com

1. INTRODUCTION

Mobile robots are used in many industrial, medical, space, and other applications. The wheeled mobile robots (WMRs) are the most widely used class of mobile robots thanks to their fast maneuverability and energy saving. In some mechanical and robotic systems, certain types of additional conditions restrict motions, such as non-integrable constraints, or in other words, nonholonomic constraints. Nonholonomic restrict the motion of robots, making them difficult to control. Under these conditions, the robot will usually not be able to move in any given path [1, 2]. For instance, WMRs, watercraft, and space robots are examples of nonholonomic systems. Such systems do not behave linearly around any of their equilibrium points and cannot be stabilized by continuously differentiable time independent feedback. The problem of stabilizing and tracking the reference path in such systems has attracted the attention of many researchers in recent years [3, 4]. As mentioned, WMRs are an example of nonholonomic systems in which the motion of WMRs is realized by actuators that determine the torque applied to the wheel and the direction of motion of the wheel axis [5]. WMRs have three degrees of freedom (DOFs) to move on the surface while having only two controllable inputs [5, 6]. One of the problems in controlling nonholonomic mobile robots is the uncertainty in modeling this system. Uncertainty in the robot is due to the inherent characteristics of the WMR, including the real dynamics of the robot, inertia, power limitation of operators, and the positioning error of the robot; hence, the equations of this system cannot be described as a simplified mathematical model [5].

Most of the controllers are dedicated to the design of a closed-loop stabilizer controller for nonholonomic mobile robots. In this case, the position of the robot must be exactly known at any moment. Nevertheless, this assumption is very unrealistic from robotics experts' point of view because a mobile robot may drift during motion. As a result, their exact location is not possible by dead reckoning alone [7]. In designing a mobile robot controller, there are two challenges: predetermined path tracking and stabilization around the desired position. In recent years, the problem of guiding WMRs with nonholonomic constraints has attracted much attention in the field of robotics [8-11]. For the problem of tracking in this system, various methods have been proposed, including proportional-integral-derivative (PID) controller [12], sliding mode controller [13, 14], neural control [15], robust adaptive control [16], fuzzy control [17], and hybrid control [18]. One of the effective methods of controlling a WMR is sliding mode control (SMC). SMC is a fruitful technique for controlling linear and nonlinear systems. This method has been widely used in systems with uncertainty due to its convenient features such as simplicity of design, acceptable consistency, reduction of order, and easy implementation. SMC and its combinations are regarded as a suitable method for robust control of systems [5, 6, 19, 20]. In [21] presents a robust control method for asymptotic stabilization of a nonholonomic mobile robot and shows that the designed sliding mode controller is robust to limited external disturbances. In [9], an SMC law was introduced to stabilize and track the reference path in nonholonomic

systems in the chain form. For limited time convergence, the terminal sliding mode control method was proposed for this system. In [22], a finite time tracking controller for nonholonomic systems is used in an extended chained form, which uses a relay switching technique and terminal sliding mode control with limited time convergence to design the controller. The authors in [23] suggest a recursive terminal sliding mode control method for tracking nonholonomic systems converted into a chained form.

Recently, a new control technique for removing the chattering problem in sliding mode controllers has been used as an excellent alternative to the saturation function method, the high-order derivative of the sliding surface, as well as other conventional approaches to removing chattering, which is a simple, robust, and practically efficient. This technique is known as "sliding mode control based on the adaptive continuous barrier function," in which an adaptive continuous barrier function is used to provide a smooth and continuous control rule for the switching surface and completely solve the chattering problem in SMC. The SMC based on the barrier function was first proposed in [24] by Franck Plestan et al. (2010) for controlling an electro-pneumatic actuator system. An adaptive continuous barrier function TSMC scheme was proposed in [25] to control a three degrees of freedom manipulator subject to external disturbances. In [26], A barrier function adaptive nonsingular TSMC approach was designed to control quad-rotor unmanned aerial vehicles with external disturbances, in which a novel nonsingular terminal sliding surface is suggested to

guarantee convergence of the sliding surface to the origin in a finite time. The work in [27] provides a quasi-adaptive sliding mode method based on the barrier function to control the motion of the hydraulic servo mechanism with modeling uncertainty. Also, barrier function-based adaptive high-order SMC has been used for the fast stabilization of a perturbed chain of integrators with bounded uncertainties [28]. Recently in [29], a TSMC based on the continuous barrier function along with a fuzzy estimator has been designed to control an inverted pendulum. The approach resulted in the creation of continuous and smooth control rules. In addition, a novel barrier function based on the adaptive technique for the first-order SMC was proposed in [30]. This technique was applied to a class of first-order disturbed systems whose upper boundaries of the uncertainty are unknown. The proposed barrier technique can guarantee the convergence of the output variables independently of the uncertainty boundaries and keep it in a neighborhood of the origin without overestimating the control gain. For this purpose, to overcome the problem caused by the upper boundaries of unknown uncertainty, the SMC method is combined with the adaptive control technique, and a novel strategy entitled "chatter-free TSMC based on adaptive continuous barrier function" is proposed. Its main contributions are as follows:

- A novel adaptive control to tune the controller's adaptation gain parameters to estimate the boundaries of the uncertainty terms.
- An adaptation gain that is not overestimated, so only the convergence of

the system state variables in a predefined neighborhood of the origin is guaranteed.

- A design that considers a barrier function as a simple switching function to completely eliminate the chattering phenomena.
- A design that guarantees the convergence and maintenance of the system state variables to a predefined neighborhood of the origin in finite time.
- A control design that covers a complete class of uncertain NWMR systems in which the upper boundaries of the uncertainty are assumed to be unknown.

The organization of this paper is as follows. In Section 2, the model of wheeled mobile robots is introduced. Section 3 designed the kinematic control law. Section 4 describes the design of the dynamic control and stability analysis. The simulation results are provided in Section 5 to evaluate the performance of the proposed controller design. Eventually, Section 6 summarizes the conclusion.

2. MOBILE ROBOT MODELING

The mobile robot in this study consists of two identical moving wheels placed on a rod so that each wheel is independently controlled by an actuator (motor) as illustrated in Fig. 1.

Referring to Fig. 1, r is the wheel radius (m), $2r$ denotes the length of the axis between actuator wheels, v_L and v_R represent the speed of the right and left wheels (m/s), (x, y) shows the position of the robot's center of gravity at any given moment. Also, θ (rad) is the angle between the axis perpendicular to the axis between the wheels of the mobile robot (x_r) and the x-axis, v is the instantaneous linear velocity, and ω gives the instantaneous angular velocity of the mobile robot body. The robot state position vector is defined as $q = (x, y, \theta)$. The angular and linear velocities of the moving robot are expressed by Eq. (1) and the equation of the kinematic model is given by Eq. (2) [31]:

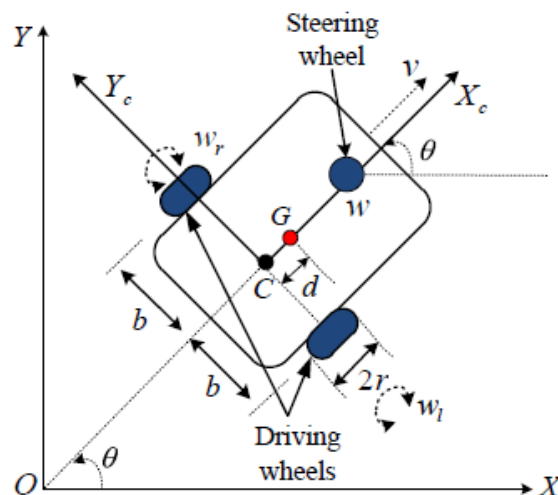


Fig. 1. The schematic model of a WMR.

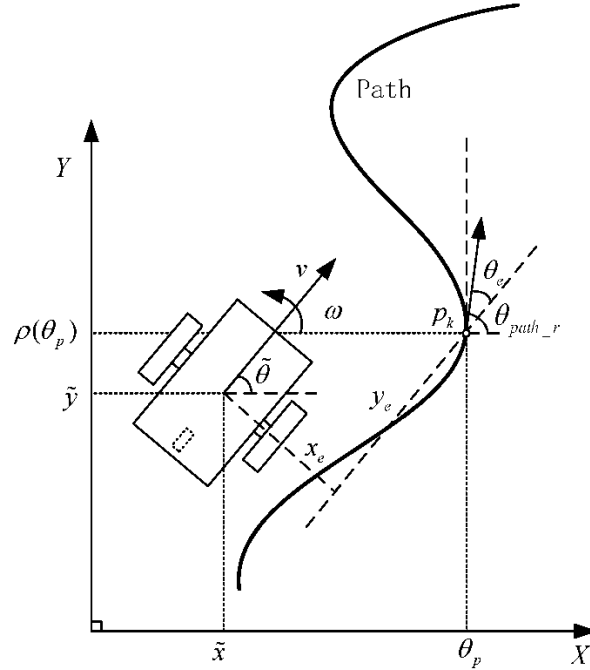


Fig. 2. The motion of virtual and real robots.

$$V = \frac{V_L + V_R}{2}, \omega = \frac{V_L - V_R}{2}$$

$$\dot{q} = \begin{bmatrix} \dot{x} \\ \dot{y} \\ \dot{\theta} \end{bmatrix} = \begin{bmatrix} \cos \theta & 0 \\ \sin \theta & 0 \\ 0 & 1 \end{bmatrix} \begin{bmatrix} V \\ \omega \end{bmatrix} \quad (1)$$

Nonholonomic constraints are assumed so that the wheels rotate without chattering. Moreover, the dynamic model of a mobile robot is presented in Eq. (3):

$$\dot{y} \cos \theta - \dot{x} \sin \theta = 0$$

$$M\dot{v}(t) - f_f(t) = F(t), \quad F(t) = \frac{\tau_L + \tau_R}{r}$$

$$I\dot{\omega}(t) - \tau_f(t) = \tau(t), \quad \tau(t) = \frac{L(\tau_L - \tau_R)}{r} \quad (2)$$

let $u_1 = \tau_L + \tau_R$, $u_2 = \tau_L - \tau_R$

where, M is the total mass of the mobile robot, I is its moment of inertia, τ_L and τ_R are motor torque of the right and left wheels, $f(t)$ represents the friction force, and τ_f indicates the friction torque, respectively.

The present paper aims to control a WMR to track a pre-designed path in the presence of uncertainty. To clarify the problem, it can be assumed that a virtual vehicle is moving on the desired reference path and the real mobile robot must follow the virtual path as shown in Fig. 2.

The position and path orientation of the virtual vehicle as well as its kinematic equations are described by Eq. (4):

$$q_d(t) = [x_d(t), y_d(t), \theta_d(t)] \quad (3)$$

$$\dot{x}_d = v_d \cos \theta_d, \quad \dot{y}_d = v_d \sin \theta_d, \quad \dot{\theta}_d = \omega_d$$

Additionally, the reference time-variant angular and linear velocities are calculated as follows:

$$\dot{V} + mV^a \leq 0 \quad (4)$$

Therefore, to find the proper control law, it is necessary that $q(t) \rightarrow q_d(t)$ as $t \rightarrow \infty$. The error between the desired position and

the real position is $e = [e_1, e_2, e_3] T = [(x - x_d), (y - y_d), (\theta - \theta_d)] T$. As a result, the error dynamics for path tracking are determined by Eq. (6):

$$t_s = t_0 + \frac{v^{1-a}(t_0)}{r(1-a)} \quad (5)$$

The control system consists of two parts. The first part is a nonlinear kinematic controller (steering) whose outputs are linear and angular velocities. The second part is a dynamic controller whose outputs are the angular and linear torques required by the robot for path tracking.

3. DESIGNING THE KINEMATIC CONTROL LAW

First, a control law for the kinematic model of a WMR is defined based on [31]:

$$v_c = \frac{v_d \cos \theta_d - \gamma e_1}{\cos \theta}, \omega_c = \omega_d - \alpha e_2 - b e_3 \quad (6)$$

where, γ , b , a are constant positive gains. v_c and ω_c are the linear and angular velocities required for kinematic stabilization, which are used as reference inputs to the dynamic control block. By placing Eq. (7) in Eq. (2) and using Eq. (6), the dynamics of the errors are obtained as follows:

$$\begin{aligned} \dot{e}_1 &= -\gamma e_1 \\ \dot{e}_2 &= -\gamma e_1 \tan \theta + \frac{v_d \sin e_3}{\cos \theta} \\ \dot{e}_3 &= -\alpha e_2 - b e_3 \end{aligned} \quad (7)$$

with selecting the Lyapunov function as follows:

$$v_e = \frac{1}{2} e_1^2 + \frac{1}{2} e_2^2 + \frac{1}{2} e_3^2 + e_2 e_3 \quad (8)$$

It is proved that the mobile robot is capable of asymptotic tracking of the reference path with error convergence to zero at $t \rightarrow \infty$ [32].

4. Dynamic control design and stability analysis

In order to obtain continuous, smooth, and differentiable control inputs and further weaken the chattering phenomenon, the idea of diverting the switching term of the discontinuous sliding surface into the first derivative of the control input is adopted. As a result, the dynamic sliding mode surfaces resulting in a smooth adaptive SMC law are defined as follows:

$$\sigma_i(t) = \dot{s}_i(t) + \lambda_i s_i(t) \quad (9)$$

where λ_i , $i=1,2,\dots,n$ are positive constants, and sliding surfaces s_i with the integral operator are defined as follows:

$$s_i(t) = k_i \int_0^t x_i(\tau) d\tau + x_i(t) \quad (10)$$

where k_i , $i=1,2,\dots,n$ are positive constants, and $x_i(t)$, $i=1,2,\dots,n$ are system state variables. The main advantage and feature of Eq. (10) is that the use of a sliding surface with this nonlinear and integral switching function makes the SMC become a global sliding mode control because the nonlinear sliding surface Eq. (10) has both GSMC conditions, i.e. $s(0)=0$ and $s(\infty)=0$. Accordingly, one of the main advantages of selecting the mentioned nonlinear and integral sliding surfaces is that the proposed

controller becomes GSMC and the phase of reaching the sliding surface is removed. This results in placing the sliding surface at the initial moment, and yielding a controller that is robust to uncertainties from the beginning.

4.1. Analysis of Stability and Convergence of System States

In the proposed control method, SMC is used to deal with the dynamic model uncertainties of the chaos system and a combination of SMC with the adaptive control approach is used to solve the upper boundaries problem of unknown model uncertainties and their estimation. In this section, we first make the following assumption to analyze the stability of system states.

Assumption 1: Here, we assume that the unknown positive constants c_i and $i=1,2,\dots,n$ exist as the upper boundaries of the system uncertainty term, so that the following inequality holds:

$$\left| \sum_{j=1}^n \frac{\partial d_i(x,t)}{\partial x_j} \dot{x}_j + \frac{\partial d_i(x,t)}{\partial t} \right| + (\lambda_i + k_i) |d_i(x,t)| \leq c_i \quad (11)$$

where $d_i(t,x)$ and $i=1,2,\dots,n$ are the unknown uncertainty terms in Eq. (1).

Note 2: Contrary to the assumption in [33], here we allow the upper boundaries of the uncertainty term, i.e., c_i , to be unknown.

$$\dot{V} = \sum_{i=1}^n \left[\begin{array}{l} \sigma_i \left(\sum_{j=1}^n \frac{\partial f_i(t,x)}{\partial x_j} \dot{x}_j + \frac{\partial f_i(t,x)}{\partial t} \right) \\ + \sum_{j=1}^n \frac{\partial d_i(t,x)}{\partial x_j} \dot{x}_j + \frac{\partial d_i(t,x)}{\partial t} + \dot{u}_i + \\ (\lambda_i + k_i)(f_i(t,x) + d_i(t,x) + u_i) + \lambda_i k_i x_i + (\hat{c}_i - c_i) \dot{\hat{c}}_i \end{array} \right], \quad (16)$$

Theorem 1: Considering assumption 1, if the adaptive TSMC rule is written as follows:

$$\begin{aligned} \dot{u}_i = & -(\lambda_i + k_i)(u_i + f_i(t,x)) \\ & - \sum_{j=1}^n \frac{\partial f_i(x,t)}{\partial x_j} \dot{x}_j + \frac{\partial f_i(x,t)}{\partial t} \\ & - \lambda_i k_i x_i - \varepsilon_i \hat{c}_i \text{sign}(\sigma_i) \end{aligned} \quad (12)$$

where $\varepsilon_i > 1$, and $i=1,2,\dots,n$ are some constant parameters related to the controller design, \hat{c}_i is the upper boundary estimate of c_i , which displays the adaption gain, and is obtained from the following equation:

$$\hat{c}_i = \varepsilon_i |\sigma_i|; \varepsilon_i > 1, \quad (13)$$

Then, for each specified initial condition, the closed-loop system state vector $x(t)$ becomes asymptotically stable, leading to the convergence of the system states to the origin.

Proof: To prove Theorem 1, consider a Lyapunov's candidate function as follows:

$$V = \frac{1}{2} \sum_{i=1}^n [\sigma_i^2 + (\hat{c}_i - c_i)^2] \quad (14)$$

Therefore, the time derivative of Lyapunov's function will be as follows:

$$\dot{V} = \sum_{i=1}^n [\sigma_i \dot{\sigma}_i + (\hat{c}_i - c_i) \dot{\hat{c}}_i] \quad (15)$$

By combining Eq. (15) with Eqs. (9) and (10), the following equation is achieved:

$$\dot{V} \leq \sum_{j=1}^n \left[\sigma_j \left(\sum_{j=1}^n \frac{\partial f_j(t, x)}{\partial x} x + \frac{\partial f_j(t, x)}{\partial t} + \dot{u}_j + (\lambda_j + k_j)(f_j(t, x) + u_j) + \lambda_j k_j x_j \right) + c_j |\sigma_j| + (\hat{c}_j - c_j) \dot{\hat{c}}_j \right] \quad (17)$$

By applying the inequality (11) of assumption 1, the following relation will be obtained in (17).

Substituting the control rule of the adaptive sliding mode (12) in inequality (17), yields the following relation:

$$\begin{aligned} \dot{V} &\leq \sum_{i=1}^n \left[-\epsilon_i \hat{c}_i \sigma_i \text{sign}(\sigma_i) \right. \\ &\quad \left. + c_i |\sigma_i| + (\hat{c}_i - c_i) \dot{\hat{c}}_i \right] \\ &= \sum_{i=1}^n \left[-\epsilon_i \hat{c}_i |\sigma_i| + c_i |\sigma_i| \right. \\ &\quad \left. + (\hat{c}_i - c_i) \epsilon_i |\sigma_i| \right] \\ &= -\sum_{i=1}^n (\epsilon_i - 1) c_i |\sigma_i| \end{aligned} \quad (18)$$

Thus, if $\epsilon_i > 1$ is selected according to the assumptions of Theorem 1, the derivative of the candidate Lyapunov function is less than or equal to zero. That is, the following inequality holds:

$$\dot{V} \leq -\sum_{i=1}^n (\epsilon_i - 1) c_i |\sigma_i| \leq 0. \quad (19)$$

Now, based on Eq. (19), we define the variable $\gamma(t)$ as the following relation:

$$y(t) = \sum_{i=1}^n (\epsilon_i - 1) c_i |\sigma_i|. \quad (20)$$

Then, by integrating both parts of (20), we will have the following inequality:

$$\int_0^t y(\tau) d\tau \leq V(0) - V(t) \leq V(0) \quad (21)$$

By taking the limits of both parts of relation (21) and considering the existence and finiteness of the limit $\int_0^t y(\tau) d\tau$, using Barbalat's lemma, the following result will be

obtained:

$$\lim_{x \rightarrow \infty} y(t) = 0 \quad (22)$$

From Eq. (22) and Eqs. (9) and (10), the following result is obtained, which means that the system states eventually converge to zero, and the closed-loop system state vector $x(t)$ is asymptotically stable.

$$\lim_{x \rightarrow \infty} \sigma_i = 0 \Rightarrow \lim_{x \rightarrow \infty} \|x(t)\| = 0 \quad (23)$$

4.2. Improvement of the Proposed Controller with Adaptive Barrier Function

In this study, to improve and develop the proposed control method, the chattering-free TSMC based on the adaptive barrier function is used for the robust stability of chaotic systems with unknown external disturbances. For this purpose, a novel adaptive control rule based on the adaptive continuous barrier function is suggested in this section. The block diagram of the proposed adaptive continuous barrier function-based chattering-free TSMC approach is illustrated in Fig.3.

Lemma 2: To improve the proposed control method, the unknown uncertainties of the system can be estimated more effectively by employing the adaptive barrier function-based TSMC, in which case the closed-loop system will be more stable. For this purpose, the adaptation gain parameter \hat{c}_i in the adaptive TSMC rule (12) can be written as follows:

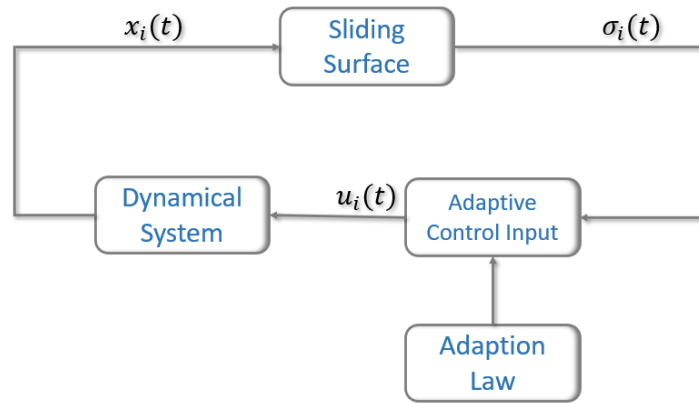


Fig. 3. Block diagram of the proposed adaptive continuous barrier function-based TSMC approach.

$$\hat{c}_i(t) = \begin{cases} \hat{c}_{i_a}(t), & \text{if } 0, t \leq \bar{t} \\ \hat{c}_{i_{psd}}(t), & \text{if } t > \bar{t} \end{cases} \quad (23)$$

where \bar{t} represents the time when the system state trajectories converge to the neighborhood τ of the sliding surface dynamics $\sigma_i(t)$, and when $t = \bar{t}$, the smallest root of the equation $|\sigma_i(t)| \leq \tau$ is obtained. In the proposed control method, the adaptation rule and positive-semi-definite (PSD) continuous barrier function are created by the following equations, respectively:

$$\dot{\hat{c}}_{i_a} = \epsilon_i |\sigma_i(t)|, \quad (24)$$

$$\hat{c}_{i_{psd}}(t) = \frac{|\sigma_i(t)|}{\tau_i - |\sigma_i(t)|} \quad (25)$$

Using where in (23), τ is a positive scalar parameter.

Note 3: The adaption rule (25) is extracted from Eq. (13) in Theorem 1.

Employing the adaptation rule (25), the adaption gain is adjusted to increase until the state trajectories reach the neighborhood τ of the sliding surface at the time \bar{t} . For times

greater than \bar{t} , the adaption gain shifts to the PSD barrier function to reduce the convergence region and hold the state trajectories in it.

For time $0 < t \leq \bar{t}$, the controller design is suggested by the control rule defined in Eq. (15) of Theorem 1, and for conditions when the time is longer than \bar{t} ($t > \bar{t}$), the controller is designed by the adaptive control rule based on the barrier function as follows:

$$\begin{aligned} \dot{u}_i = & -(\lambda_i + k_i)(u_i + f_i(t, x)) \\ & - \sum_{j=1}^n \frac{\partial f_i(t, x)}{\partial x_j} \dot{x}_j - \frac{\partial f_i(t, x)}{\partial t_j} - \lambda_i k_i x_i - \epsilon_i \hat{c}_{i_{psd}}^{(26)} \text{sign}(\sigma_i) \end{aligned}$$

Then, the system state trajectories reach the convergence region $|\sigma_i(t)| \leq \tau$ in a finite time. As a result, the system state trajectories converge to the origin in a finite time, and the closed-loop system will reach stability in a finite time.

Note 4: The process of designing and generating adaptive control rules (12) and (27) according to the method [33] is briefly illustrated in Appendix A.

Note 5: According to lemma 2, using the

adaptive barrier function in the SMC, the proposed controller will be automatically finitetime; in other words, the closed-loop control system will be stable in a finite time.

Proof: The controller stability with the control rule (12) was proven in the previous subsection. Here again, the proof is based on Lyapunov's approach and is shown according to [33] that the system state trajectories reach the convergence region $|\sigma_i(t)| \leq \tau$ in a finite time. To prove the controller stability with the control rule (27), we can consider a Lyapunov's candidate function which includes both sliding surface dynamics and adaption gain dynamics (barrier function), as follows:

$$V_i(t) = 0.5 \left(\sigma_i(t)^2 + (\hat{c}_{i_{psd}}(t) - \hat{c}_{i_{psd}}(0))^2 \right) \quad (27)$$

Taking the time derivative of the Lyapunov's function (28), yields:

$$\dot{V}_i(t) = (\sigma_i(t)\dot{\sigma}_i(t) + (\dot{\hat{c}}_{i_{psd}}(t) - \dot{\hat{c}}_{i_{psd}}(0))) \quad (28)$$

Substituting the sliding surface derivative $\dot{\sigma}_i(t)$ and $d(0)=0$ in Eq. (29), yields:

$$\begin{aligned} \dot{V}_i(t) = & \sigma_i(t) \left[\sum_{j=1}^n \frac{\partial f_i(t,x)}{\partial x_j} \dot{x}_j + \frac{\partial f_i(t,x)}{\partial t} \right. \\ & + \sum_{j=1}^n \frac{\partial d_i(t,x)}{\partial x_j} \dot{x}_j + \frac{\partial d_i(t,x)}{\partial t} + \dot{u}_i + (\lambda_i + k_i) \left(f_i(t,x) + d_i(t,x) + u_i \right) \\ & \left. + \lambda_i k_i x_i \right] + \dot{\hat{c}}_{i_{psd}}(t) \hat{c}_{i_{psd}}(t), \end{aligned} \quad (29)$$

Applying the inequality (11) of assumption 1 and placing the control input u_i of Eq. (27) in Eq. (30) yields:

$$\begin{aligned} \dot{V}_i(t) = & \sigma_i(t) \left(-\epsilon_i \hat{c}_{i_{psd}}(t) \operatorname{sgn}(\sigma_i(t)) \right. \\ & \left. + d(t,x) + \hat{c}_{i_{psd}}(t) \dot{\hat{c}}_{i_{psd}}(t) \right) \\ \leq & |\sigma_i(t)| \times \left\{ |d(t,x) - \epsilon_i \hat{c}_{i_{psd}}(t)| \right\} \\ & + \hat{c}_{i_{psd}}(t) \dot{\hat{c}}_{i_{psd}}(t) \quad (30) \\ \leq & |\sigma_i(t)| \times \left\{ |d(t,x) - \epsilon_i \hat{c}_{i_{psd}}(t)| \right\} + \hat{c}_{i_{psd}}(t) \\ \times & \frac{\tau}{(\tau - |\sigma_i(t)|)^2} \\ & \left[|d(t,x) - \epsilon_i \hat{c}_{i_{psd}}(t) \operatorname{sgn}(\sigma_i(t))| \right] \\ \times & \operatorname{sgn}(\sigma_i(t)) \end{aligned}$$

From Eq. (31), the following inequality can be obtain:

$$\dot{V}_i(t) \leq - \left\{ \epsilon_i \hat{c}_{i_{psd}}(t) - |d(t,x)| \right\} |\sigma_i(t)| - \hat{c}_{i_{psd}}(t) \times \frac{\tau}{(\tau - |\sigma_i(t)|)^2} \left[\epsilon_i \right. \quad (31)$$

Since from (32), an upper boundary can be found as follows:

$$\begin{aligned} \dot{V}_i(t) \leq & -\sqrt{2} \left\{ \epsilon_i \hat{c}_{i_{psd}}(t) - |d(t,x)| \right\} \frac{|\sigma_i(t)|}{\sqrt{2}} \\ & - \frac{\sqrt{2}\tau}{(\tau - |\sigma_i(t)|)^2} \left[\epsilon_i \hat{c}_{i_{psd}}(t) - |d(t,x)| \right] \\ & \frac{\hat{c}_{i_{psd}}(t)}{\sqrt{2}} \quad (32) \\ \leq & -Z \left(\frac{|\sigma_i(t)|}{\sqrt{2}} + \frac{\epsilon_i \hat{c}_{i_{psd}}(t)}{\sqrt{2}} \right) \leq -Z V_i(t)^{0.5} \end{aligned}$$

where:

$$Z = \sqrt{2} \left\{ \epsilon_i \hat{c}_{i_{psd}}(t) - |d(x,t)| \right\} \min \left\{ 1, \frac{\sqrt{2}\tau}{(\tau - |\sigma_i(t)|)^2} \right\} \quad (33)$$

Therefore, due to Eq. (33) and according to Lyapunov's stability theorem and lemma 2,

we can conclude that the proposed control system will be stable in a finite time.

5. SIMULATION RESULTS

To show the effectiveness of the proposed control design, the system is simulated in the MATLAB software and its performance is compared with conventional multivariate PI controllers and the Terminal sliding mode control (TSMC) presented in [28]. The suitable trajectory is $y = g(x) = \sin(0.5x) + 0.5x + 1$ and the path's image on the x-axis is

$x(t) = t$. The model input for desirable linear and angular velocities are generated as illustrated in Fig. 3. The robot parameters are quantified as given in Fig. 1:

$$m = 9kg, r = 1m, I = 5kg/m^2, L = 2m$$

We consider the disturbance term as follows:

$$d(t, x) = \begin{bmatrix} \sin(x_1) \\ \sin(t) \\ \sin(x_1) + \sin(t) \end{bmatrix} \quad (34)$$

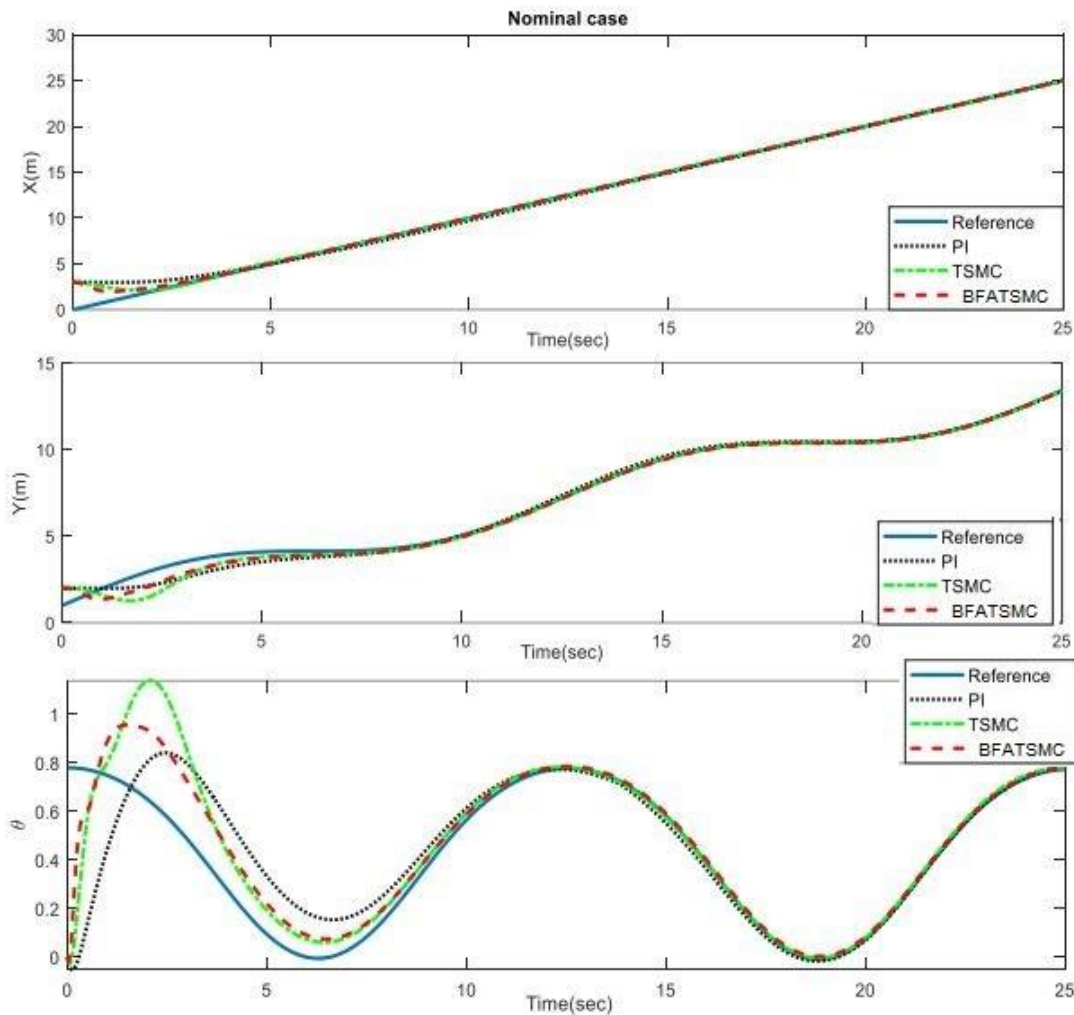


Fig. 4. Close-loop system responses. Up: along the x-axis, middle: along the y-axis, and down: head angle of the robot.

Table 1. Design parameters of PI, TSMC, and FO-NTSMC controllers.

| | BFTSMC | | TSMC | | | PI | |
|----------|--------|-------|------|-------|------|----------|-------|
| α | 0.9 | k_1 | 5 | Y | 1 | K_{p1} | 13.97 |
| ρ | 0.1 | k_2 | 2 | k_1 | 1.79 | K_{p2} | 14.01 |
| δ | 0.1 | y_1 | 20 | k_2 | 2.63 | K_{I1} | 0.45 |
| a_1 | 2 | y_2 | 1 | C_1 | 0.5 | K_{I2} | 0.43 |
| a_2 | 1.8 | | | C_2 | 1 | | |

In the first scenario, robot simulation is carried out without considering frictionless and uncertainty for the determined path tracking. Also, it is assumed that the mobile robot starts with initial speeds of $v(0) = 0$ and $\omega(0) = 1$ and the initial position of $q = [3, 2, 0] T$, while the desired path starts from the point $qd = [0, 1, 0.78] T$. Design parameters of three PI, TSMC, and BFATSMC controllers are tabulated in Table 1. It should be noted that the objective criterion of the Integral Squared Error (ITS) has been optimized by a genetic algorithm (GA) to adjust the coefficients of these controllers.

Figs. 4 and 5 present responses of PI, TSMC, and BFATSMC controllers for WMR path tracking in the presence of a large error in the initial position and the absence of disturbance. The first and second images in Fig. 5 illustrate the robot's behavior along the x- and y axes, and the third image describes the head angle behavior of the robot. It is clear that the WMR's response caused by all mentioned controllers tracks the desired path after 10 seconds.

Fig. 5 depicts the behavior of angular and linear speed errors converging to zero. As one can observe, the response error caused by the proposed BFATSMC controller is faster than

the PI and TSMC controllers in converging to zero and shows less overshoot. These results verify the suitable efficiency and high tracking performance of the suggested controller than PI and TSMC controllers.

Fig. 6 shows the control effort signal established by PI, TSMC, and BFATSMC controllers to track the reference input. The magnitude of the control effort signal of BFATSMC is greater than PI and TSMC controllers during the transient period. The reason is that the control rule related to this controller requires a huge control effort to ensure tracking of the desirable path.

To ensure that a system has suitable performance, the controller needs to be appropriately coordinated with the system. The controller design aims to tune its parameters in a way that the error caused by perturbation or changing the adjustment point disappears rapidly with the minimum variations. The speed of error elimination and ensuring the minimum overshoot is measured using a criterion function in terms of time and error. To this end, the Integral Squared Error (ITS) and the Integral of Time Multiply Squared Error (ITSE) functions are calculated for all three above-mentioned controllers, and the related results are listed in Table 2.

Table 2 clearly illustrates the BFATSMC controller performs the other PI and TSMC controllers in tracking the desired path based on ISE and ITSE error criteria. Moreover, concerning the above evaluation criteria, it is observed that the overshoot in the transient response of the BFATSMC controller is smaller than that of PI and TSMC controllers. The oscillations of this controller are mitigated more rapidly and the path is tracked

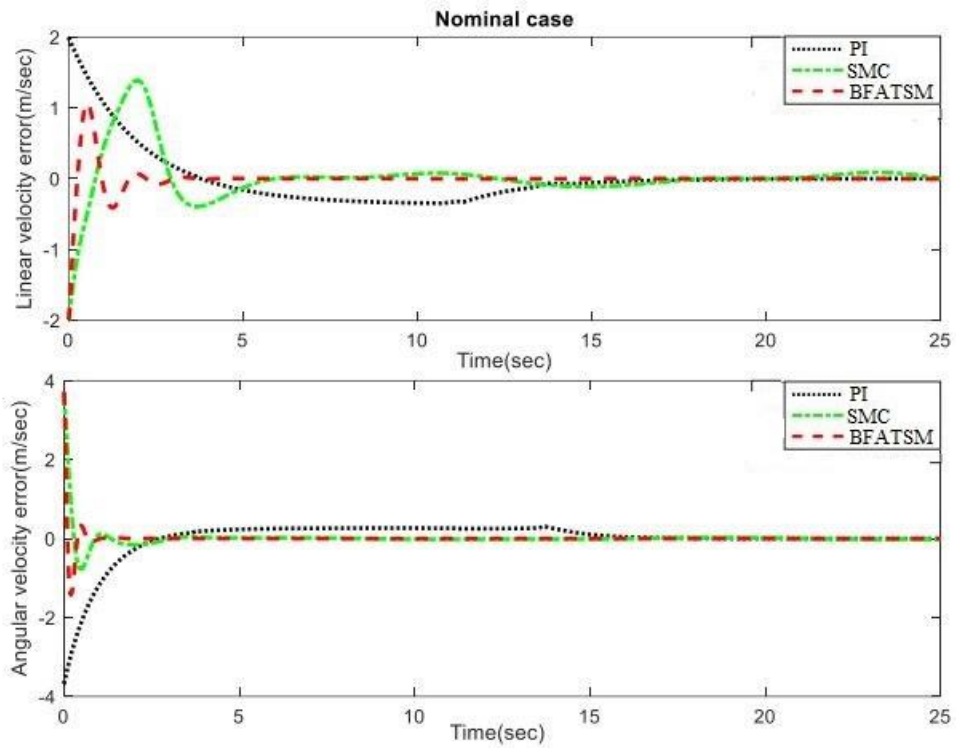


Fig. 5. Up: Tracking error of linear forward velocity, down: tracking error of angular velocity.

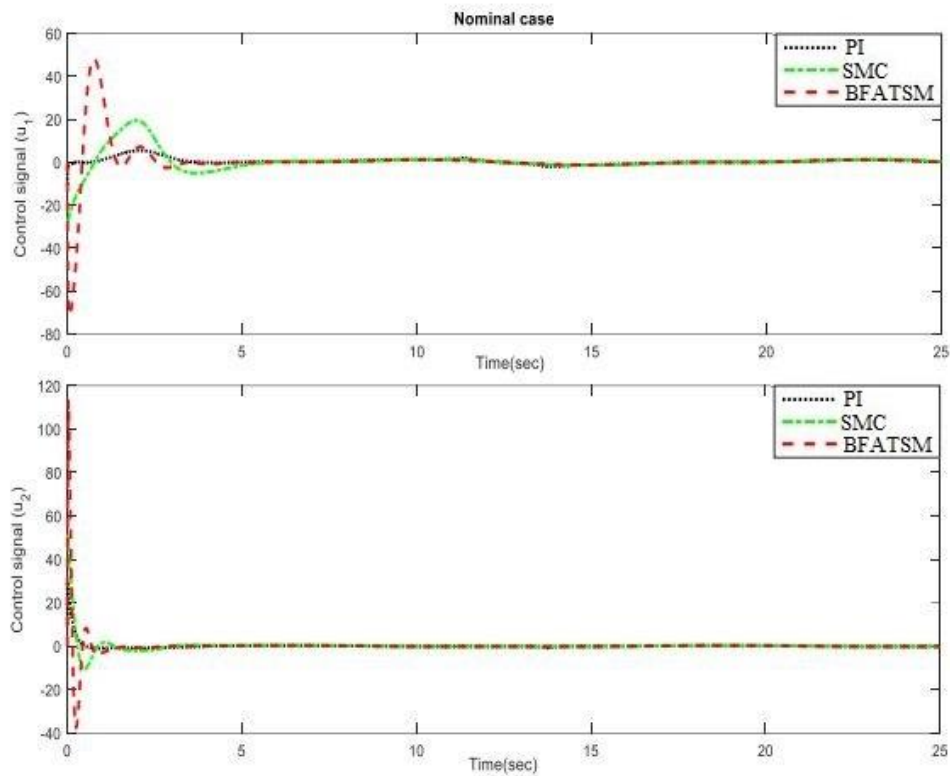


Fig. 6. Up: magnitude of the control signal u_1 ; down: magnitude of the control signal u_2 .

Table 2. A comparison between the performance of PI, TSMC, and BFATSMC controllers based on error criterion functions.

| Angular velocity error | | Linear velocity error | | Control method |
|------------------------|--------|-----------------------|--------|----------------|
| ITSE | ISE | ITSE | ISE | |
| 717.843 | 1596.3 | 526.67 | 602.43 | PI |
| 36.06 | 917.81 | 318.39 | 447.89 | TSMC |
| 15.0848 | 789.96 | 30 | 303.62 | FO-NTSMC |

without any steady error. In this scenario, limited uncertainty and an external disturbance are applied to the robot system to validate the robustness of the proposed controller. To this end, the mass and inertia of the robot have been changed by 10% with respect to their nominal values. Also, the friction force and the torque caused by friction set $f = 2N$ and $\tau f = 2N$. m , respectively. The desired path and initial conditions of the robot are similar to the previous scenario. Fig. 6 demonstrates the behavior of angular and linear velocity errors

caused by the mentioned controllers in the presence of uncertainty and disturbance. These results verify that uncertainty has degraded the quality of the response of PI and TSMC controllers and led to increased tracking error. However, the proposed BFATSMC controller succeeds in dealing with the adverse effects of model uncertainty and disturbance and maintains its efficiency. Thus, it can be concluded that path tracking by the proposed controller is considerably robust to parameter uncertainties and external disturbances.

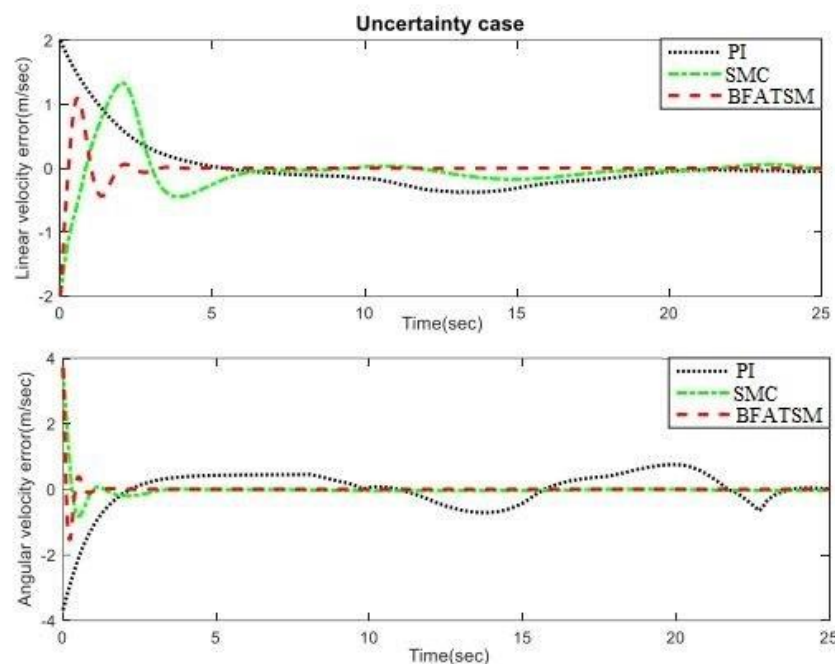


Fig. 7. Up: linear velocity error and, down: angular velocity error.

6. CONCLUSION

This paper presents a novel control design for a WMR, which includes nonlinear dynamic and kinematic models of the robot. Furthermore, in this approach, the path tracking problem was applied to a nonholonomic mobile robot. The nonlinear nonholonomic model of the robot is controlled by using the fractional-order nonsingular terminal sliding mode control to achieve the target position on the desired optimal path. A simple mathematical law was proposed to select the feedback gains of controller switching in different initial conditions. The robot successfully tracked the reference path using the proposed approach. Based on the obtained results, the suggested technique has been effective because the tracking error has converged to zero in a limited time. Additionally, this approach is compared with the sliding mode control approach presented in [28] and the typical multivariate PI control. The results show that the proposed control robot follows the desired path with very few steady-state errors in the presence of parametric uncertainty. Therefore, the proposed control is more accurate than the conventional sliding mode control and the multivariate PI control. Eventually, the results prove the efficiency, simplicity, and accuracy of the proposed control strategy.

REFERENCES

- [1] Falsafi, M., K. Alipour, and B. Tarvirdizadeh, *Fuzzy motion control for wheeled mobile robots in real-time*. Journal of Computational & Applied Research in Mechanical Engineering (JCARME), 2019. 8(2): p. 133-144.
- [2] Murray, R.M. and S.S. Sastry, *Nonholonomic motion planning: Steering using sinusoids*. IEEE Transactions on Automatic Control, 1993. 38(5): pp. 700-716.
- [3] Cui, D. and H. Li, *Model predictive control of nonholonomic mobile robots with backward motion*. IFAC-PapersOnLine, 2019. 52(24): p. 195-200.
- [4] Mobayen, S., *Fast terminal sliding mode tracking of non-holonomic systems with exponential decay rate*. IET Control Theory & Applications, 2015. 9(8): p. 1294-1301.
- [5] Yang, J.-M. and J.-H. Kim, *Sliding mode control for trajectory tracking of nonholonomic wheeled mobile robots*. IEEE Transactions on robotics and automation, 1999. 15(3): p. 578-587.
- [6] Nikranjbar, A., M. Haidari, and A.A. Atai, *Adaptive sliding mode tracking control of mobile robot in dynamic environment using artificial potential fields*. Journal of Computer & Robotics, 2018. 11(1): p. 1-14.
- [7] Reis, M.F., et al., *Robust moving path following control for robotic vehicles: Theory and experiments*. IEEE Robotics and Automation Letters, 2019. 4(4): p. 3192-3199.
- [8] Nguyen, T., K. Nguyentien, and P.T. Do T, *Neural network-based adaptive sliding mode control method for tracking of a nonholonomic wheeled mobile robot with unknown wheel slips, model uncertainties, and unknown bounded external disturbances*. Acta

- Polytechnica Hungarica, 2018. 15(2): p. 103-23.
- [9] DUMLU, A. and M.R. YILDIRIM, *Real-time implementation of continuous model based sliding mode control technique for trajectory tracking control of mobile robot*. Balkan Journal of Electrical and Computer Engineering, 2018. 6(4): p. 211-216.
- [10] Xu, Q., et al., *Fuzzy PID based trajectory tracking control of mobile robot and its simulation in Simulink*. International journal of control and automation, 2014. 7(8): p. 233-244.
- [11] Salem, F.A., *Dynamic and kinematic models and control for differential drive mobile robots*. International Journal of Current Engineering and Technology, 2013. 3(2): p. 253-263.
- [12] Lee, C.-T. and W.-T. Sung, *Controller design of tracking WMR system based on deep reinforcement learning*. Electronics, 2022. 11(6): p. 928.
- [13] Filipescu, A., et al. *Trajectory-Tracking Sliding-Mode Control of the Autonomous Wheelchair Modeled as a Nonholonomic WMR*. in *2018 IEEE 14th International Conference on Control and Automation (ICCA)*. 2018. IEEE.
- [14] Nath, K., et al., *Event-triggered sliding-mode control of two wheeled mobile robot: an experimental validation*. IEEE Journal of Emerging and Selected Topics in Industrial Electronics, 2021. 2(3): p. 218-226.
- [15] Korayem, M.H., H.R. Adriani, and N.Y. Lademakhi, *Regulation of cost function weighting matrices in control of WMR using MLP neural networks*. Robotica, 2023. 41(2): p. 530-547.
- [16] Fang, H., et al., *Robust tracking control for magnetic wheeled mobile robots using adaptive dynamic programming*. ISA transactions, 2022. 128: p. 123-132.
- [17] Chwa, D. and J. Boo, *Adaptive fuzzy output feedback simultaneous posture stabilization and tracking control of wheeled mobile robots with kinematic and dynamic disturbances*. IEEE Access, 2020. 8: p. 228863-228878.
- [18] Kamel, M.A., X. Yu, and Y. Zhang, *Real-time fault-tolerant formation control of multiple WMRs based on hybrid GA-PSO algorithm*. IEEE Transactions on Automation Science and Engineering, 2020. 18(3): p. 1263-1276.
- [19] Koubaa, Y., M. Boukattaya, and T. Dammak, *Adaptive sliding-mode dynamic control for path tracking of nonholonomic wheeled mobile robot*. Journal of Automation and Systems Engineering, 2015. 9(2): p. 119-131.
- [20] 20. Yang, F., et al., *Adaptive and sliding mode tracking control for wheeled mobile robots with unknown visual parameters*. Transactions of the Institute of Measurement and Control, 2018. 40(1): p. 269-278.
- [21] Liu, Y., et al., *Autonomous Planning and Robust Control for Wheeled Mobile Robot With Slippage Disturbances Based on Differential Flat*. IET Control Theory & Applications, 2023. 17(16): p. 2136-2145.
- [22] Li, S., et al., *Adaptive NN-based finite-*

- time tracking control for wheeled mobile robots with time-varying full state constraints*. Neurocomputing, 2020. 403: p. 421-430.
- [23] Moudoud, B., H. Aissaoui, and M. Diany. *Finite-time adaptive trajectory tracking control based on sliding mode for Wheeled Mobile Robot*. in *2021 18th International Multi-Conference on Systems, Signals & Devices (SSD)*. 2021. IEEE.
- [24] Plestan, F., et al., *New methodologies for adaptive sliding mode control*. International journal of control, 2010. 83(9): p. 1907-1919.
- [25] Mobayen, S., K.A. Alattas, and W. Assawinchaichote, *Adaptive continuous barrier function terminal sliding mode control technique for disturbed robotic manipulator*. IEEE Transactions on Circuits and Systems I: Regular Papers, 2021. 68(10): p. 4403-4412.
- [26] Alattas, K.A., et al., *Barrier function adaptive nonsingular terminal sliding mode control approach for quad-rotor unmanned aerial vehicles*. Sensors, 2022. 22(3): p. 909.
- [27] Dong, Z. and J. Ma, *Quasi-Adaptive sliding mode motion control of hydraulic servo-mechanism with modeling uncertainty: a barrier function-based method*. IEEE Access, 2020. 8: p. 143359-143365.
- [28] Chitour, Y., et al., *Barrier Function-Based Adaptive Continuous Higher-Order Sliding Mode Controllers with Unbounded Perturbations*. arXiv preprint arXiv:2206.10904, 2022.
- [29] Sepestanaki, M.A., et al., *Fuzzy estimator indirect terminal sliding mode control of nonlinear systems based on adaptive continuous barrier function*. IEEE Access, 2022. 10: p. 34296-34305.
- [30] Obeid, H., et al., *Barrier function-based adaptive sliding mode control*. Automatica, 2018. 93: p. 540-544.
- [31] Latombe, J.-C., *Robot motion planning*. Vol. 124. 2012: Springer Science & Business Media.
- [32] Ailon, A., N. Berman, and S. Arogeti, *On controllability and trajectory tracking of a kinematic vehicle model*. Automatica, 2005. 41(5): p. 889-896.
- [33] Li, H., et al., *Chaos control and synchronization via a novel chatter free sliding mode control strategy*. Neurocomputing, 2011. 74(17): p. 3212-3222.